Multimedia Tools and Applications (2019) 78:25685–25706
https://doi.org/10.1007/s11042-019-07792-x

Corner detection based on tangent-to-point distance accumulation technique

Shizheng Zhang[1] · Sheng Huang[2,3] · Zhifeng Zhang[1] · Heng Wang[4] · Junxia Ma[1] · Pu Li[1]

Received: 5 August 2018 / Revised: 15 March 2019 / Accepted: 15 May 2019 /
Published online: 31 May 2019

Abstract

The core of the contour-based corner detection is essentially performing a good curvature estimation on planar curves. Inspired by intuitive observation that the curvature of a point on a contour is proportional to the distance accumulation of its neighbors to the tangent of the point, we present a novel curvature estimator named Relative Tangent-to-Point Distance Accumulation (RTPDA) for contour-based corner detection. In the approach, we fit the curve segments with quadratic polynomials by employing least square technique to derive the tangent of the target point, and then accumulate the distance of its neighbors to the tangent, which is a good approximation of the discrete curvature. Experiments verify the effectiveness and the efficiency of the proposed detector in comparison with several influential corner detectors under three commonly used evaluation metrics, namely, Average Repeatability (AR), Localization Error (LE) and Accuracy index (ACU).

Keywords Least square fitting · Discrete curvature · Corner detection · Repeatability · Localization error

✉ Sheng Huang
huangsheng@cqu.edu.cn

[1] Software Engineering College, Zhengzhou University of Light Industry, Zhengzhou 450000, People's Republic of China

[2] Ministry of Education Key Laboratory of Dependable Service Computing in Cyber Physical Society, Chongqing 400044, People's Republic of China

[3] School of Big Data & Software Engineering, Chongqing University, Chongqing 400044, People's Republic of China

[4] College of Mechanical and Electrical Engineering, Henan Agricultural University, Zhengzhou 450000, China

1 Introduction

Corners are widely applied for helping to tackle many tasks in image processing and computer vision communities, such as 3D construction, object tracking, robot navigation, and image registration. By now, extensive corner detection approaches have been proposed. Generally speaking, these methods can be categorized into two groups [29]: Intensity-based and contour-based. Intensity-based methods [1, 2, 10–13, 15, 21, 25, 27, 28] directly deal with the intensity values (or grey scales) while contour-based methods [4, 5, 9, 14, 16, 17, 23, 26, 29–38] directly or indirectly estimate a significance measure (e.g., curvature) on the points of a planar curve, and select the curvature extrema points as corners [29]. Our approach follows the latter.

With respect to the contour-based corner detectors, curvature estimation is the crucial step [6] and by now lots of influential curvature estimation methods have been proposed. Among them, some corner detectors estimate the curvature of a plane curve directly according to its mathematic definition. For example, the curvature scale-space (CSS) [23], ATCSS [14] and multi-scale curvature product (MSCP) [32] calculated the plane curvature K as follows:

$$\mathrm{K}(\mathrm{u},\sigma)=\frac{\dot{X}(u,\sigma)\ddot{Y}(u,\sigma)-\ddot{X}(u,\sigma)\dot{Y}(u,\sigma)}{\left[\dot{X}(u,\sigma)^2+\dot{Y}(u,\sigma)^2\right]^{1.5}} \tag{1}$$

where $\dot{X}(u,\sigma)=x(u)\otimes\dot{\mathrm{g}}(u,\sigma)$, $\ddot{X}(u,\sigma)=x(u)\otimes\ddot{\mathrm{g}}(u,\sigma)$, $\dot{Y}(u,\sigma)=y(u)\otimes\dot{\mathrm{g}}(u,\sigma)$, $\ddot{Y}(u,\sigma)=y(u)\otimes\ddot{\mathrm{g}}(u,\sigma)$, and $\otimes$ is the convolution operator. $\mathrm{g}(u,\sigma)$ denotes a Gaussian function with deviation σ, and $\dot{\mathrm{g}}(u,\sigma)$, $\ddot{\mathrm{g}}(u,\sigma)$ are the first and second derivatives of $\mathrm{g}(u,\sigma)$ respectively. $x(u)$ and $y(u)$ are the coordinate functions controlled by the given parameter u. This curvature estimation technique is sensitive to the local variation and noise due to its small region of support (RoS) [4, 6]. Meanwhile, many other corner detectors estimate plane curvature via presenting lots of "discrete curvature" which can reflect the degree of the curvature of planar curves. For example, Rosenfeld etc. (RJ73) [26] treated angle as discrete curvature; Awrangjeb and Lu etc. employed the Chord-to-Point Distance Accumulation for discrete curvature estimation [4]. Other "discrete curvatures" include eigenvalue [30], eigenvector [31], GCM [33] and KD curvature [9], SODC [16], ACRA [17] and so on. It has been concluded in [6] that the second kind of approaches enjoy more robustness and higher performance in general. A review of the relevant review works on contour-based corner detection methods can be found in [6, 24].

There are two major problems faced by contour-based corner detectors. One problem is that they heavily rely on the edge-detection results. Different edge detection methods will yield different contours which will greatly reflect the corner detection results. The other problem is that they are sensitive to noise and geometric transformations. For the first problem, robust contour extraction schemes should be proposed; for the second one, constructing robust curvature estimators is an effective way. We are devoted to tackle the second problem. Inspired by intuitive observation that the curvature of a point on a contour is positively correlated to the distance accumulation of its neighbors to the tangent of the point, we present a novel corner detector based on the *Relative Tangent-to-Point Distance Accumulation* (RTPDA) technology. Since RTPDA uses a relatively larger neighborhood without using any derivative based measurements, it is less sensitive to noise compared with CSS-based corner detectors. What's more, by adopting relative distance for estimation, RTPDA is more robust to the uniform scaling transform.

The rest of paper is organized as follows. The related works were presented in section 2. In Section 3, we discuss the motivation and the methodology of the proposed corner detection approach. Section 4 presents the image datasets and evaluation metrics employed in this paper. Section 5 presents the experimental results and we present the conclusion in Section 6.

2 Related works

In this section, we shortly review the chord-to-point distance accumulation (CPDA) technique which is the most relevant work [4]. Let a chord move along a curve, CPDA detector estimates the "discrete curvature" of a point p_t on the curve with the summation of the perpendicular distances from p_t to the chord. Figure 1 illustrates the basic idea of CPDA technique and eq. (2) presents the measurement of the CPDA curvature under one RoS.

$$h_L(t) = \sum_{j=t-L+1}^{t-1} d_{t,j} \tag{2}$$

where j denotes the index of the first intersected point between chord and curve, every time the chord moves. Three curvature functions$h_1(t)$, $h_2(t)$ and $h_3(t)$ are calculated corresponding to three chords of lengths $L_1 = 10$, $L_2 = 10$ and $L_3 = 10$. Three functions are normalized as

$$h_j'(t) = \frac{h_j(t)}{\max\left(abs\left(h_j\right)\right)}, \text{for} \quad 1 \le t \le n \text{ and } 1 \le j \le 3 \tag{3}$$

Then the discrete curvature values range from 0 to 1. Finally, the three normalized curvature functions $h_j'(t)$ are multiplied together to find a single curvature value.

$$H(t) = h_1'(t)h_2'(t)h_3'(t), \text{for } 1 \le t \le n \tag{4}$$

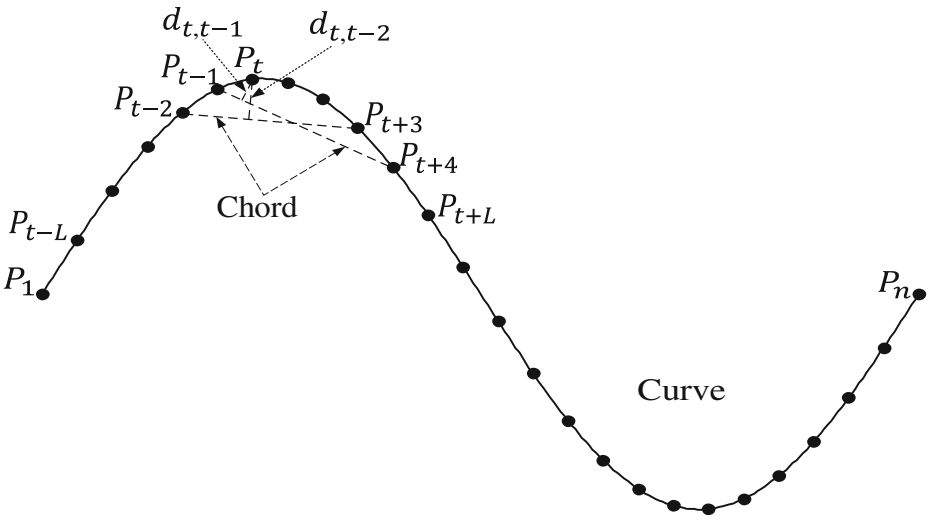

Fig. 1 Chord-to-point distance accumulation technique for a chord of length $L = 10$

With respect to CPDA detector, discrete curvature is calculated with the chord-to-point distance accumulation, while discrete curvature is calculated with the tangent-to-point distance accumulation in our proposed RTPDA detector. Moreover, there are some other differences between these detectors. CPDA detector uses a larger radius. This may make it miss some weak corners. And it also utilizes the maximum normalization, which can result in the false reflection of the curvature of contour in some situations [17]. In contrast, RTPDA adopts relative a small radius which alleviates this problem. With regard to the computational complexity, CPDA corner detector utilizes three normalized curvature functions to calculate the corner response value, which is quite time-consuming [17], while RTPDA just uses one region of support and experimental results also empirically show that RTPDA is faster than both CPDA and Fast-CPDA. The comparative characteristics of CPDA and RTPDA are summarized in Table 1.

3 Methodology

In this section, we first specify the motivation of the proposed curvature estimation method and then analyze the relationship between the estimated curvature and real curvature.

3.1 Motivation of RTPDA

We illustrate the basic idea of our proposed method by an intuitive example. Figure 2 shows two parabolic curves $y = x^2$ and $y = 3x^2$ that are both tangent to x axis at the origin $p_0 = (0, 0)$. It is not hard to derive the curvature at p_0 of the curve $y = 3x^2$ is 6 which is larger than the one of the curve $y = x^2$. Meanwhile, it is also not hard to find that the heights of the neighbors of p_0 on the curve $y = 3x^2$ to x axis is higher than those on the curve $y = x^2$. Since x axis is the tangent line of both the two curves at p_0, we can find that the curvature at p_0 is positively related with the distance of its neighbors to the tangent. In the following, we will further explain the relationship under more general conditions.

3.2 Related to curvature

In differential geometry of curves, the osculating circle S of a sufficiently smooth plane curve C at a given point p is the one among all tangent circles at the point p that approaches the curve most tightly. The curvature of C at p is defined as the curvature of that circle and the curvature is just the same as the reciprocal of the radius of the circle. In the following, to simplify the analysis, we substitute an arc of the osculating circle at the target point for a small fragment of C centered at the point, which can help us study the relationship between the real curvature and the estimated curvature.

Table 1 Comparative characteristics of CPDA and RTPDA detectors

Difference	CPDA	RTPDA
Distance	Point to chord	Point to tangent
Curve smoothing	Multi-scale	Single-scale
RoS	Large (10, 20 and 30)	Small (4 or 6)
Time efficiency	Time-consuming	Fast

Let us consider the following circle S_R: $x^2 + (y - R)^2 = R^2$ shown in Fig. 3a. It is easy to find that S_R passes through the origin and the radius of S_R is R. The tangent line of S_R at the origin is the x axis. Assume the point $p_0 = (x_0, y_0)$ is on S_R, there is ${x_0}^2 + (y_0 - R)^2 = R^2$. If p_0 is near enough to the origin, we have $y_0 = R - \sqrt{R^2 - {x_0}^2}$. The distance of p_0 to the x axis equals to y_0. With some derivations, we have $y_0 = \frac{{x_0}^2}{R + \sqrt{R^2 - {x_0}^2}} = \frac{\frac{1}{R}}{1 + \sqrt{1 - \left(\frac{1}{R}\right)^2 {x_0}^2}} {x_0}^2$. Keep x_0 fixed, y_0 increases monotonically with $\frac{1}{R}$, which means that the larger the curvature at the origin is, the longer distance from the point near the origin to the tangent line (x axis) at the origin. The relationship between the length and $\frac{1}{R}$ is shown in Fig. 3b.

Given a target point on a plane curve, we get that the distance of its neighbor to the tangent line of the curve at the point increases with the curvature at the point. So we can use the distance as discrete curvature estimation at the target point. However, the distance is proportional to uniform scaling, which means it is not robust to that transformation. Such behavior indicates that it needs choosing different thresholds for different scaled images based on one same original image. To make the distance more robust under the uniform scaling, we alternatively use the ratio of the distance to the length of the chord from the target point to its neighbor. The derived relative distance can be represented by

$$d_r = \frac{y_0}{\sqrt{{x_0}^2 + {y_0}^2}} = \sqrt{\frac{1}{2}} \frac{\frac{1}{R} x_0}{\sqrt{1 + \sqrt{1 - \left(\frac{1}{R}\right)^2 {x_0}^2}}}, \tag{5}$$

which also increases monotonically with $\frac{1}{R}$. The relationship of the relative distance and the $\frac{1}{R}$ is shown in Fig. 3c. In the next step we construct our curvature estimator at the origin according to the following scheme: 1) assign the region of support (RoS) of the origin (target point); 2) for every point on the RoS, we calculate a relative distance described as above; 3) the accumulation of all the relative distances is considered as the discrete curvature estimation at the origin. The reason why we use the distance accumulation is that more neighbors of the target point can participate in the calculation of the curvature at the target point in this way, and a relative bigger neighborhood is robust to noise in general.

3.3 Relative tangent-to-point distance accumulation

In the following, we present a novel "discrete curvature" estimation technique based on the above described basic idea. Let m sequential digital points describe a contour $\boldsymbol{C}$, $\boldsymbol{C} = \{p_j = (x_j, y_j), j = 1, 2, \cdots, m\}$, where p_{j+1} is adjacent to p_j. Denote $N_k(p_i)$ as a small boundary segment of $\boldsymbol{C}$, which is defined by the RoS between points p_{i-k} and p_{i+k} for some integer k, i.e. $N_k(p_i) = \{p_j | j = i - k, \cdots, i + k\}$. Our aim is to calculate the "discrete curvature" at the point p_i. The first step is calculating the tangent line at p_i. To achieve this aim, we parameterize the $2k + 1$ points and can get two parameterized point sets $\{(j,\ x_{i+j})\}_{j=-k}^{k}$ and $\left\{\left(j,\ y_{i+j}\right)\right\}_{j=-k}^{k}$. According to the least squares criterion, we

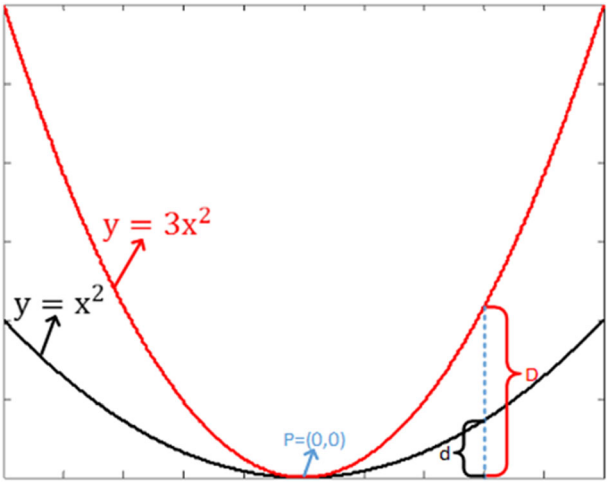

Fig. 2 An intuitive illustration of the main idea of the proposed RTPDA detector

respectively fit the polynomial series:$\mathrm{x}(\mathrm{t}) = \sum_{n=0}^{2}\alpha_n t^n$and $\mathrm{y}(\mathrm{t}) = \sum_{n=0}^{2}\beta_n t^n$, to the point sets $\{(j,\ x_{i+j})\}$ and $\{(j,\ y_{i+j})\}$, where $j = -k, \cdots, -1, 1, \cdots, k$, $\mathrm{x}(0) = x_i$ and $\mathrm{y}(0) = y_i$.The coefficients $\boldsymbol{\alpha} = (\alpha_0,\ \alpha_1,\ \alpha_2)$ and $\boldsymbol{\beta} = (\beta_0,\ \beta_1,\ \beta_2,)$ are estimated as follows:

$$\boldsymbol{\alpha} = \underset{\boldsymbol{\alpha}}{\operatorname{argmin}} \sum_{j=-k,j\neq 0}^{k} \left(\mathrm{x}(j) - x_{i+j}\right)^2, \mathrm{s.t}\ \mathrm{x}(0) = x_i \tag{6}$$

$$\boldsymbol{\beta} = \underset{\boldsymbol{\beta}}{\operatorname{argmin}} \sum_{j=-k,j\neq 0}^{k} \left(\mathrm{y}(j) - y_{i+j}\right)^2, s.t\ \mathrm{y}(0) = y_i \tag{7}$$

By solving the above two optimization problems with constraints, we have

$$\alpha_1 = \frac{\sum_{j=-k,j\neq 0}^{k} x_{i+j} - x_i j}{\sum_{j=-k,j\neq 0}^{k} j^2} = \frac{3}{k(k+1)(2k+1)} \sum_{j=-k,j\neq 0}^{k} x_{i+j} - x_i j \tag{8}$$

$$\beta_1 = \frac{\sum_{j=-k,j\neq 0}^{k} y_{i+j} - y_i j}{\sum_{j=-k,j\neq 0}^{k} j^2} = \frac{3}{k(k+1)(2k+1)} \sum_{j=-k,j\neq 0}^{k} y_{i+j} - y_i j \tag{9}$$

The tangent line of $\boldsymbol{C}$ at $\boldsymbol{p_i}$ is determined by the target point $\boldsymbol{p_i}$ and the direction (α_1, β_1). For any point $\boldsymbol{p} = (x, y)$ on $\boldsymbol{C}$, its distance to the tangent line at $\boldsymbol{p_i}$ is represented by

$$\left| \frac{\beta_1 (x - x_i) - \alpha_1 (y - y_i)}{\sqrt{\alpha_1^2 + \beta_1^2}} \right| \tag{10}$$

Divided by $\left|\overrightarrow{pp_i}\right| = \sqrt{(x-x_i)^2 + (y-y_i)^2}$, we can derive its relative distance as follow

$$\frac{1}{\sqrt{\alpha_1^2 + \beta_1^2}} \left| \frac{\beta_1 (x-x_i) - \alpha_1 (x-y_i)}{\sqrt{(x-x_i)^2 + (x-y_i)^2}} \right| \tag{11}$$

then the accumulation of the relative distances among the RoS between points p_{i-k} and p_{i+k} is represented by

$$\frac{1}{\sqrt{\alpha_1^2 + \beta_1^2}} \sum_{\substack{j=-k \\ j \neq 0}}^{k} \left| \frac{\beta_1 \left(x_{i+j} - x_i\right) - \alpha_1 \left(y_{i+j} - y_i\right)}{\sqrt{\left(x_{i+j} - x_i\right)^2 + \left(y_{i+j} - y_i\right)^2}} \right| \tag{12}$$

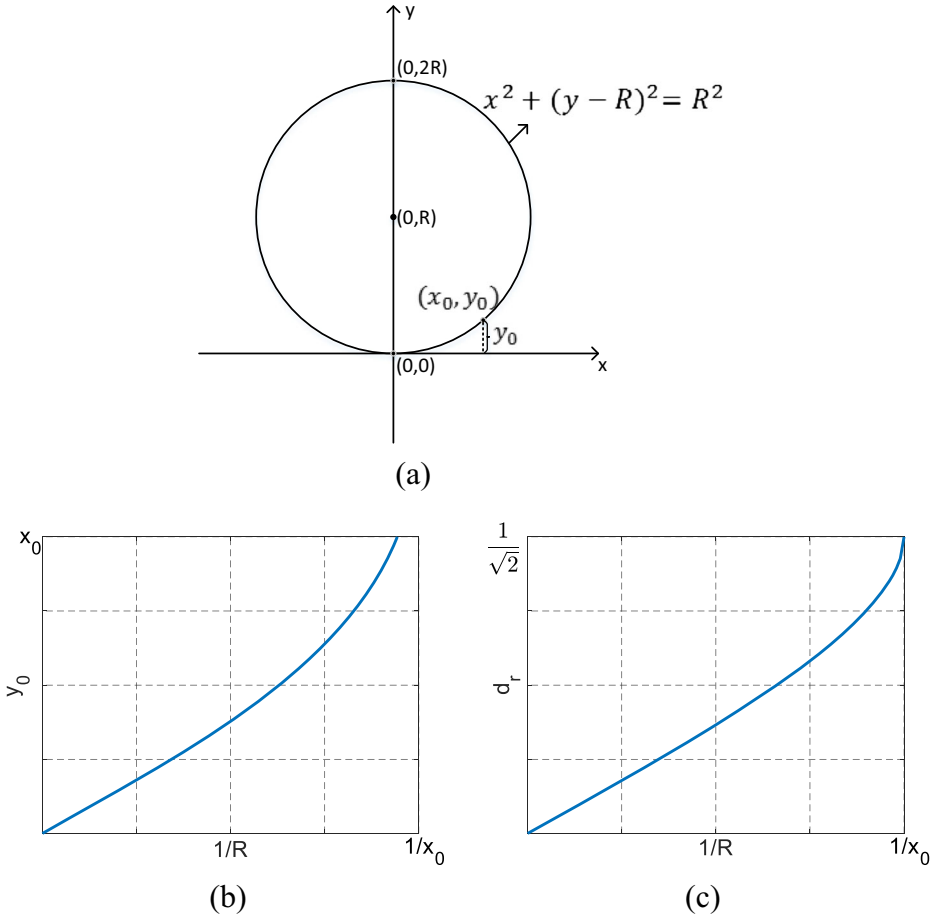

Fig. 3. **a** The showing of the circle 꾇 ;(**b**) the changing of 뚕$_0$ with variable $\frac{1}{R}$; (**c**) the changing of 꾇 with variable $\frac{1}{R}$

which is used as the "discrete curvature" of $\boldsymbol{C}$ at $\boldsymbol{p_i}$ in this paper. We named our proposed detector as Relative Tangent to Point Distance Accumulation (RTPDA) detector. The whole procedure is shown in the following algorithm.

Algorithm: Relative Tangent-to-Point Distance Accumulation

Inputs: gray-scale image, standard derivation (σ), radius of support region (RoS) and Threshold (T).

Outputs: corners of the gray-scale image.

Step 1: extract and select contours from the original gray image.

Step 2: fill gaps and locate the T-junctions and mark them as T-corners in the edge contours.

Step 3: find the corners for any extracted contour $\boldsymbol{C} = \{(x(n), y(n))\}_{n=1}^{N}$, where $x(n)$ and $y(n)$ denote coordinate functions. In detail, do step

step 4: Smooth $\boldsymbol{C}$ by convolution with Gaussian function $\mathrm{G}(u, \sigma) = \frac{1}{\sqrt{2\pi}\sigma}\exp(-\frac{u^2}{2\sigma^2})$, the smoothed version of $\boldsymbol{C}$ can be represented as $\boldsymbol{C}(\sigma) = \{(x(n,\sigma), y(n,\sigma))\}_{n=1}^{N}$, where $x(n,\sigma) = x(n) \otimes G(n,\sigma)$, $x(n,\sigma) = y(n) \otimes G(n,\sigma)$.

Step 5: calculate the discrete curvature at $\mathrm{p}(\mathrm{n},\sigma) = (x(n,\sigma), y(n,\sigma))$ as $K(n,\sigma)$ according to equation (12).

Step 6: Retain those points $\mathrm{p}(\mathrm{n},\sigma)$, where $K(n,\sigma) > K(m,\sigma)$ for all m such that $|n-m| \leq 2$ and $K(n,\sigma) \geq T$ as corner points.

Step 8: output the all saved corners.

4 Image datasets and evaluation metrics

4.1 Image datasets

In this section, two image datasets are adopted to evaluate the performance of the compared corner detectors. The images from Dataset 1 shown in Fig.4 can be found in [33] while the images from Dataset 2 shown in Fig.5 are provided by Dr. M. Awrangjeb [3]. Many images from Dataset 1 are simple binary images which contains little gray

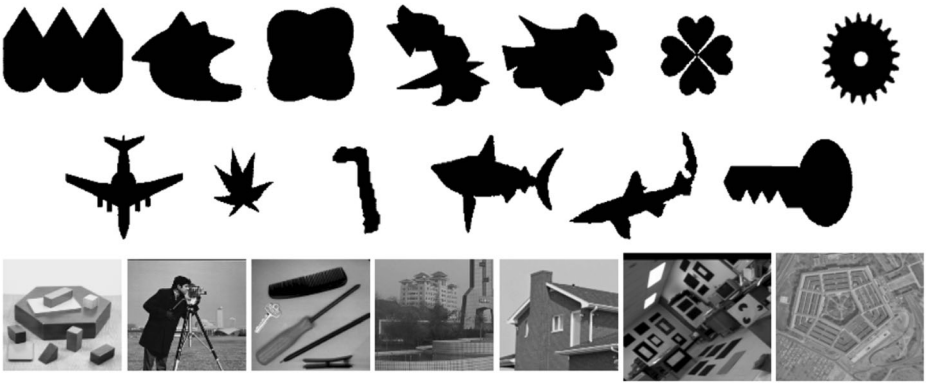

Fig. 4 The sample images from the Dataset 1

information while the images of Dataset 2 are all gray-scale images. The transformed images of the two datasets are considered as test images, which were obtained by applying the five different types of experiments on each original image described as follows:

1) Rotation: The original image was rotated with rotation angles chosen by uniform steps of interval $[-90^o, \ +90^o]$ at a 10^o resolution.
2) Uniform scaling: The original image was zoomed with scale factors chosen by uniform scaling of the interval$[0.5, 2]$ at a resolution of 0.1.
3) Non-uniform scaling: scaling factors s_x in [0.7, 1.5] and s_y in [0.5, 1.8], at 0.1 apart.
4) Combined transformations (rot.-scale): θ in $[-30^o, +30^o]$ at 10^o apart, followed by uniform or non-uniform scaling factors s_x and s_y in [0.8 1.2] at 0.1 apart.
5) Gaussian noise: Gaussian white noise with zero-mean and variances was introduced to the original image chosen by uniform sampling of the intervals $[0.005, 0.05]$. Distance between consecutive samples was 0.005.

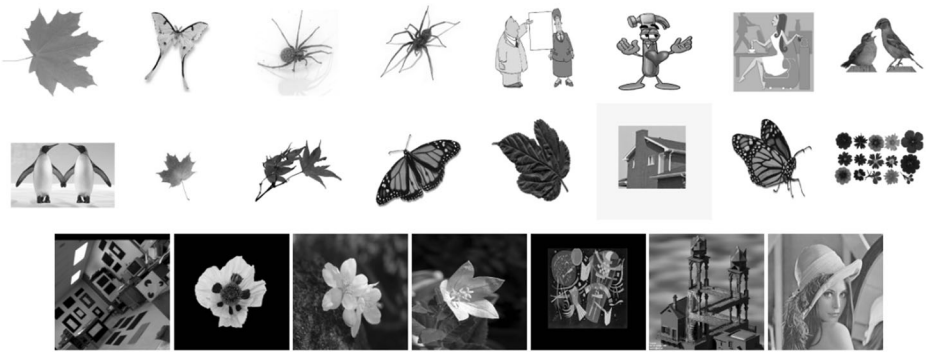

Fig. 5 The sample images from the Dataset 2

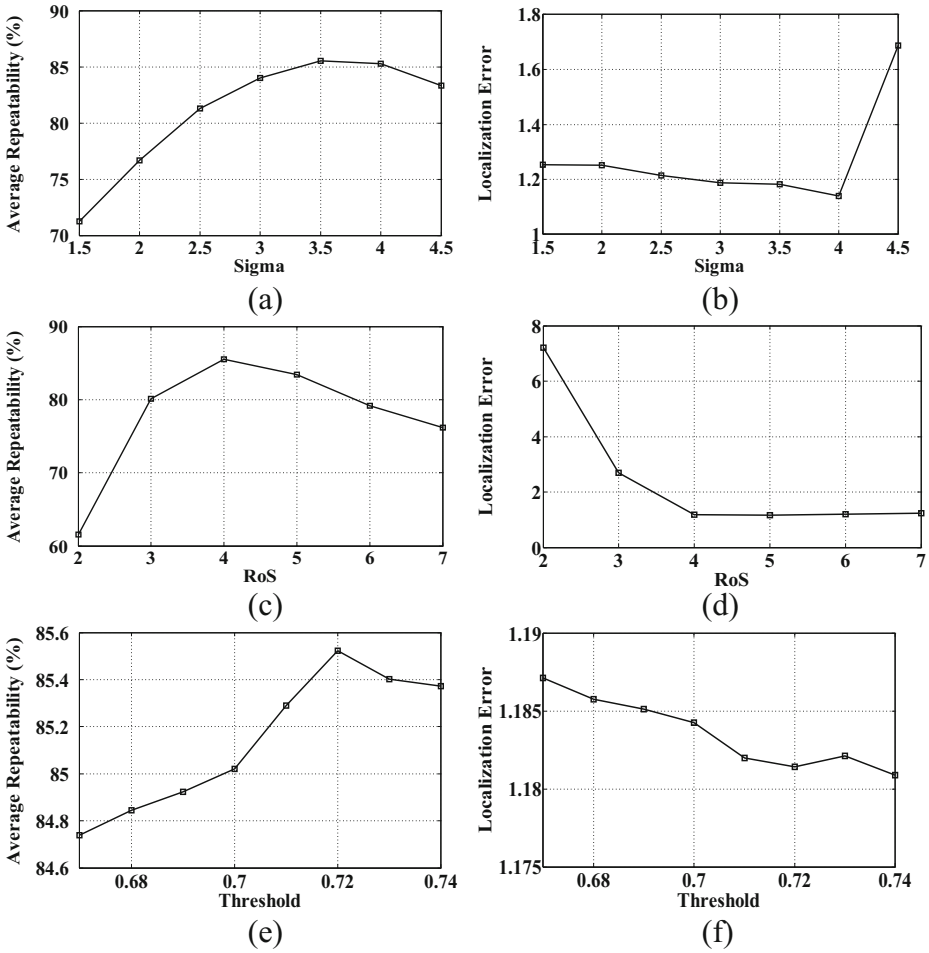

Fig. 6 Effects of different parameter changes (Gaussian smoothing scale, RoS and curvature threshold) on the RTPDA corner detector

4.2 Evaluation criteria

We use two criteria to evaluate performance. The one criterion is average repeatability (AR) [4] and localization error (LE); the other one is accuracy (ACU) [22] and localization error (LE).

4.2.1 Average repeatability and localization error

(a) Average Repeatability

Let N_o and N_T be the number of corners detected from an original image and its transformed image respectively. N_r is the number of repeated corners in the original image and transformed image. Then AR can be represented as

Table 2 Parameters of the compared detectors

Detectors(Reference)	Sigma	Radius	Threshold	
			Dataset 1	Dataset 2
RTPDA	3.5	4	0.72	0.85
CTAR [29]	3	3	0.993	0.99
SODC [16]	1,3,5	7	0.015	0.023
LoG [36]	3.5	–	0.016	0.016
CPDA [4]	1,2,3	10,20,30	0.2, 158^0	0.2, 159^0
F-CPDA [5]	3,4	10,20,30	0.2, 157^0	0.2, 159^0
GCM [33]	3	1	0.007	0.007
MSCP [32]	2,2.5	–	0.017	0.02
Eigenvector [31]	3	10	0.2	0.23
RJ73 [26]	3	$0.1 \times L_C$	–	–

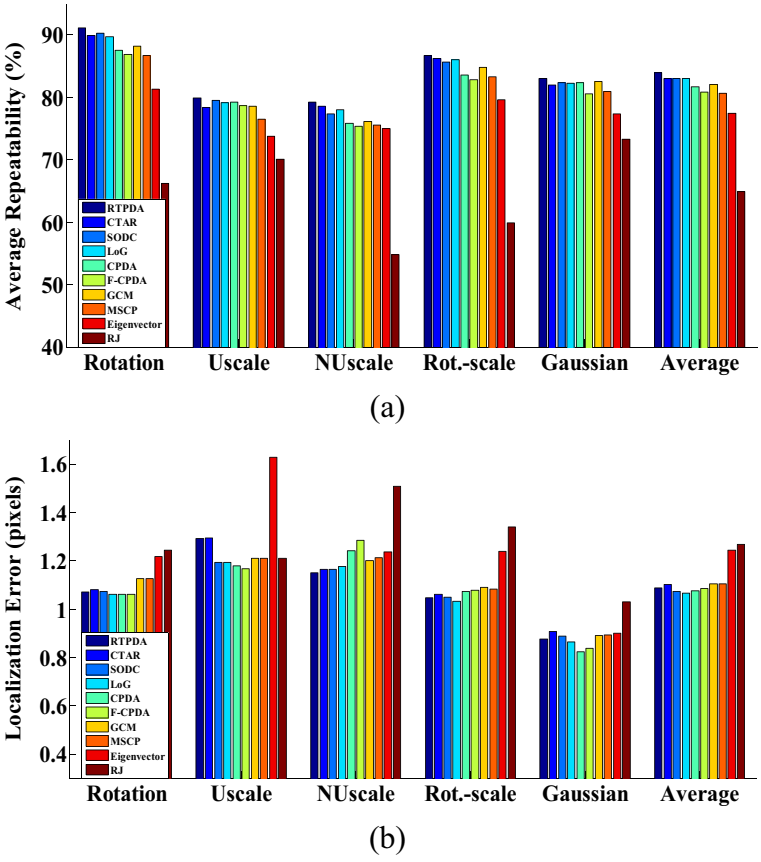

Fig. 7 Comparative results under geometric transformations using Dataset 1. (**a**) Average Repeatability and (**b**) Localization Error

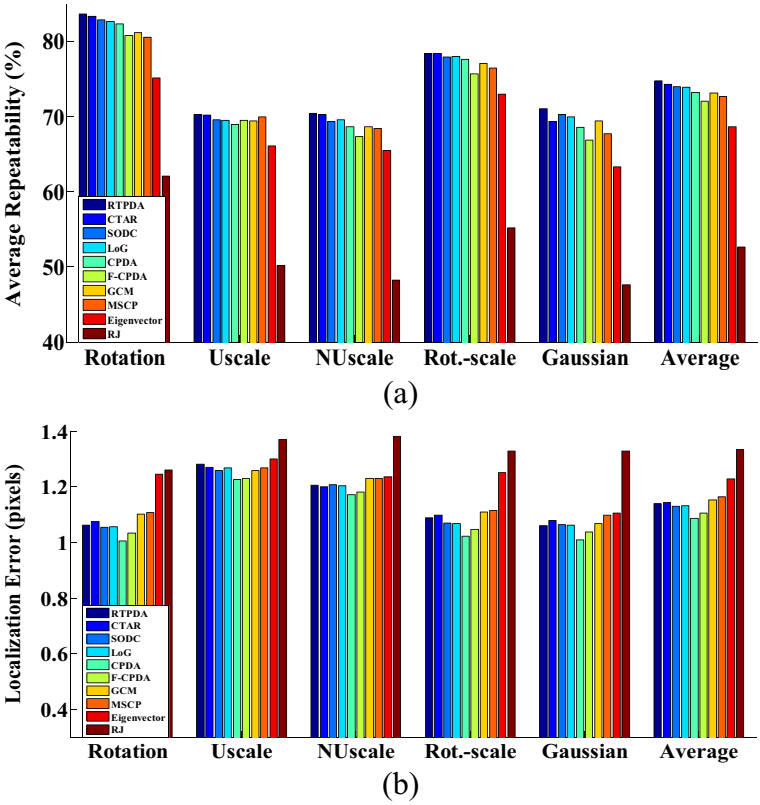

Fig. 8 Comparative results under geometric transformations using Dataset 2. (**a**) Average Repeatability and (**b**) Localization Error.

$$R_a = \frac{N_r}{2}\left(\frac{1}{N_o} + \frac{1}{N_T}\right) \tag{13}$$

(b) Localization Error

The localization error in this criterion is measured as the Root-Mean-Square-Error (RMSE) of the detected corners

$$L_e = \sqrt{\frac{1}{N_r}\sum_{i=1}^{N_r}\left[(x_{ti}-x_{oi})^2 + (y_{ti}-y_{oi})^2\right]} \tag{14}$$

Where (x_{oi}, y_{oi}) and (x_{ti}, y_{ti}) are the original position and the test position of the ith repeated corner respectively. An RMSE value of maximal 3 pixels was allowed to find a corner correspondence or repetition.

As two commonly used metrics, Repeatability mainly measures the stability of a corner detector while LE measures the accuracy of a corner detector.

Table 3 The performances of the compared detectors

Detectors	AR(Percentage)		LE(pixels)	
	Dataset 1	Dataset 2	Dataset 1	Dataset 2
RTPDA	**84.01**	**74.76**	1.09	1.14
CTAR	83.05	74.32	1.10	1.14
SODC	83.07	74.00	1.07	1.13
LoG	83.07	73.94	**1.07**	1.13
CPDA	81.72	73.24	1.08	**1.09**
F-CPDA	80.87	72.02	1.09	1.11
GCM	82.09	73.15	1.10	1.15
MSCP	80.64	72.63	1.11	1.16
Eigenvector	77.44	68.62	1.24	1.22
RJ73	64.89	52.66	1.27	1.33

The bold ones indicate the best performance under that evaluation metric

4.2.2 Accuracy and localization error

(a) Accuracy

Let N_o, N_g, and N_a be the number of detected corners, "ground truth" corners and correctly matched corners respectively, accuracy (ACU) can be represented as

$$ACU = \left(\frac{N_a}{N_o} + \frac{N_a}{N_g}\right)/2 \times 100\% \tag{15}$$

(b) Localization Error

Let N_r be the number of correctly matched corners between the test image and reference image, LE is defined as the Root-Mean-Square-Error (RMSE)

Table 4 Total times to detect corners on Dataset 1 and Dataset 2 with different corner detectors (average results over ten random experiments)

Ranks	Total execution time (s)		
	Detectors	Dataset 1	Dataset 2
1	CTAR	0.0380	0.0676
2	SODC	0.0491	0.0934
3	RTPDA	0.0545	0.1027
4	F-CPDA	0.0757	0.1263
5	LoG	0.0859	0.1491
6	MSCP	0.1194	0.2055
7	GCM	0.1296	0.2282
8	CPDA	0.1731	0.2931
9	RJ73	0.5921	0.8992
10	Eigenvector	0.7474	1.7905

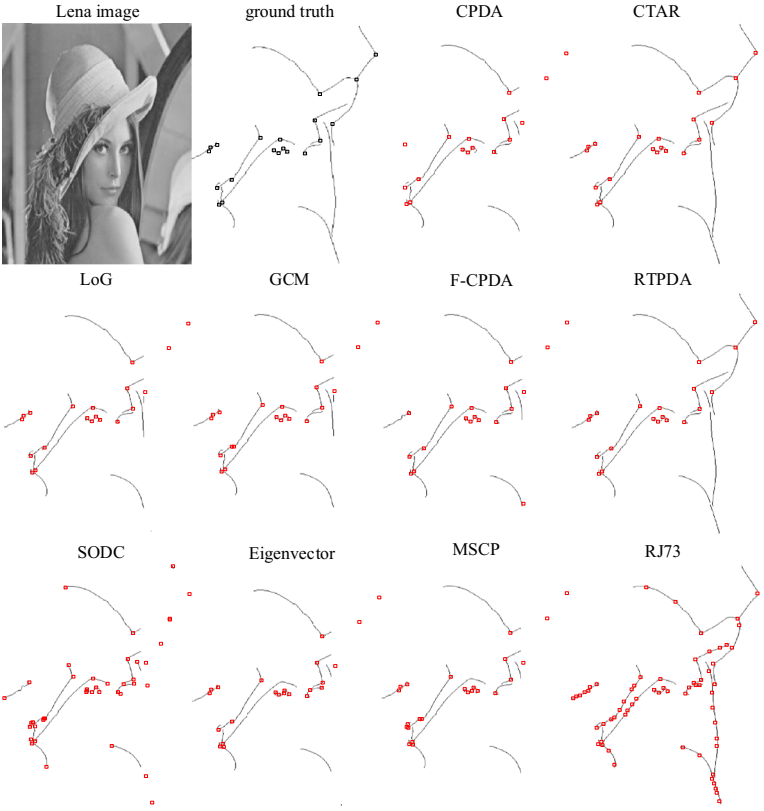

Fig. 9 Corners of "Lena" detected by ten contour-based corner detectors

$$LE = \sqrt{\frac{1}{N_r}\sum_{i=1}^{N_r}\left[\left(x_{gi}-x_{ti}\right)^2 + \left(y_{gi}-y_{ti}\right)^2\right]} \tag{16}$$

where $(x_{gi},\ y_{gi})$ is the position of the ith matched corner in the reference image and $(x_{ti},\ y_{ti})$ is that in the test image.

Since accuracy index (ACU) involves human visual inspection procedure, it is hard to implement for proper robustness tests in practice [6].

Table 5 Parameters of the compared detectors

Detectors(Reference)	Sigma	Radius	Threshold Dataset 1
RTPDA	3	4	0.74
CTAR [29]	3	3	0.993
SODC [16]	1,3,5	7	0.012
CPDA [4]	1,2,3	10,20,30	0.04, 160^0
GCM [33]	3	1	0.004

Table 6 The performances of the compared detectors

Detectors	ACU(Percentage) Dataset 1	LE(pixels) Dataset 1
RTPDA	**72.50**	1.44
CTAR	72.26	1.44
SODC	71.84	1.44
CPDA	70.46	1.47
GCM	70.41	1.45

5 Experiment results and discussion

In this section, some experiments are conducted to evaluate RTPDA detector compared with the-state-of-art corner detectors in two aforementioned criteria. These approaches are included: i) LoG [36], ii) CTAR [29], iii) GCM [33], iv) CPDA [4], v) F-CPDA [5], vi) MSCP [32], vii) Eigenvector [31], viii) RJ73 [26], ix) SODC [16].

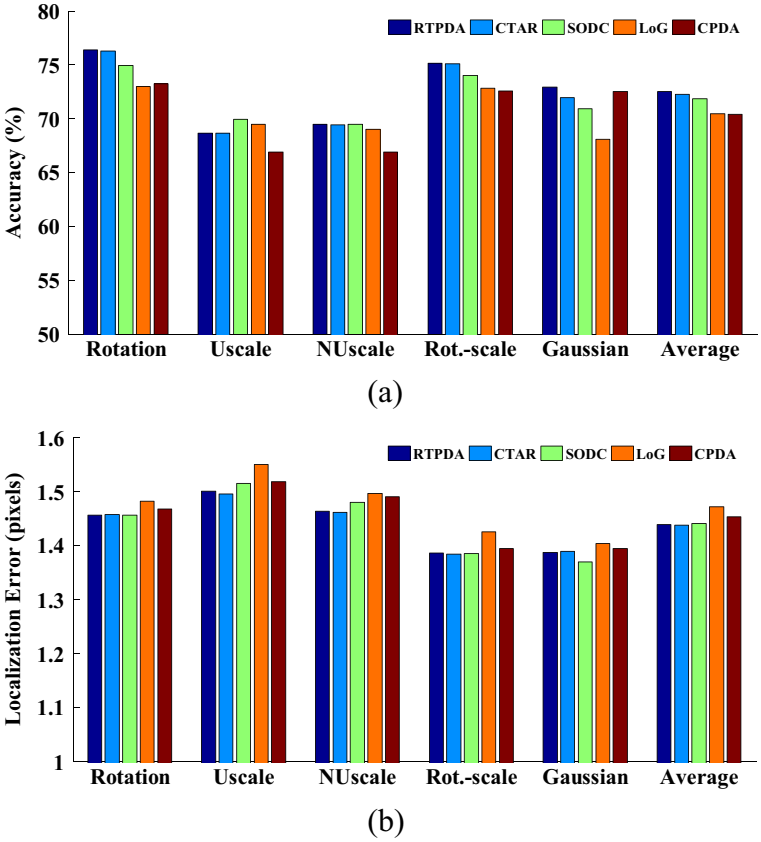

Fig. 10 Comparative results under geometric transformations using Dataset 1. (a) Accuracy and (b) Localization Error

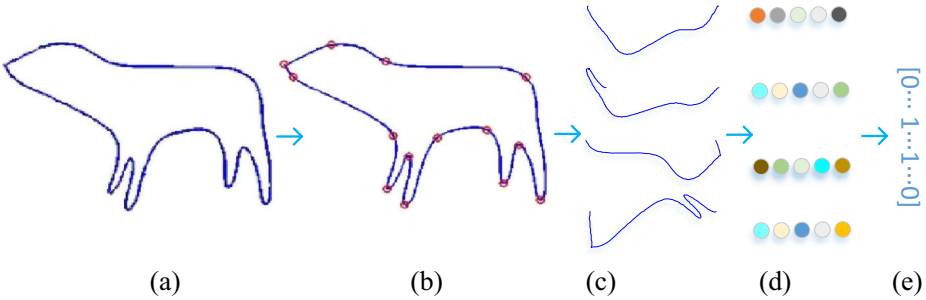

Fig. 11 An example of building shape representation using corners (**a**) contour of a shape; (**b**) corners detected using RTPDA method; (**c**) some contour fragments of the shape divided by corners; (**d**) contour fragment descriptions; (**e**)we use K-means clustering algorithm to acquire the codebook of the contour fragments and then can derive the shape representation

5.1 Performance evaluation based on repeatability criterion

5.1.1 Parameter selection

The behaviors of RTPDA detector changing along with the parameters setting are analyzed in this section and we mainly consider three parameters: (1) Gaussian smoothing scale (σ), (2) RoS (n), and (3) curvature threshold (*T*). We conduct several experiments to empirically select the optimal parameter.

Figure 6 shows the effect of different parameters (Gaussian smoothing scale σ, the size of RoS n and curvature threshold *T*) to the performances of the RTPDA. In this experiment, we tune one parameter at one time and keep the others fixed. It should be noted that the parameters of the other compared detectors have also been well tuned. We present the selected parameters of all the compared methods in Table 2 and the performances are reported in Figs. 7 and 8, and Table 3 in detail. Canny edge detector [8] is chosen as the contour tracking method and its parameters are set following the ones in [4, 6]. For a fair comparison, the same Canny edge extraction and contour-tracking methods are applied for all comparative detectors.

5.1.2 Performance evaluation

Figure 7 and 8 show the results under different geometric transformations and Gaussian noise on Dataset 1 and Dataset 2, respectively. Overall, the proposed RTPDA detector shows the highest average repeatability in all datasets, with a similar localization error as the one of the CTAR detector. RTPDA detector used both a relative big neighborhood and large scale factor, which can improve its robustness to the geometric transformations and Gaussian noise. LoG detector had better localization (lower error) compared with other nine well-known detectors on Dataset 1 while CPDA detector [6] had better localization on Dataset 2. GCM detector performed not well as the recent proposed LoG and CTAR detectors, it was pointed out in [13] that it used a very small neighborhood (1×1) and its significance measure is highly sensitive to geometric transformation. Since Eigenvector detector [31] calculated the discrete curvature by utilizing the wavelet transform of contour orientation, it was sensitive to noise too. Without adopting any derivative of curve-point locations RTPDA has not suffered from this drawback. SODC [16] is a recently proposed corner detector by employing simple triangular theory and distance calculation. Since it utilized absolute distance instead of relative distance, it was not as

robust as RTPDA in some geometrical transformations such as uniform scaling or non-uniform scaling. In all, RTPDA provided promising performances in term of AR and LE for two datasets demonstrating its effectiveness in corner finding. However, we noticed that RTPDA performed not so well in LE metric. Its localization error is somewhat high. We attribute this to the fact that RTPDA adopts a large Gaussian smoothing scale to remove noise. In this situation Multi-scale technique may be a suitable choice for RTPDA considering its good performance on suppressing noise and improving localization [16, 32].

5.1.3 Time efficiency

We tabulate the computational time of each evaluated detector on Dataset 1 and Dataset 2 in Table 4. All the experiments are conducted in a Win10 machine with 3.4 GHz Intel(R) Core(TM) Quad CPU and 8GB of RAM (Matlab-2012b). It should be noted that the time for curve extraction is not included in the total computational costs since it is identical for every compared detector. CTAR runs fastest by estimating discrete curvature with only three points based on triangle theory while Eigenvector runs slowest due to the time-consuming wavelet transform. RTPDA is faster than fast-CPDA detector, which also reveals its high efficiency.

Figure 9 shows some visualization results, with the corners of "Lena" image detected by the nine testing algorithms. The "ground truth" corners of "Lena" image can be referred to [6]. We can see that the proposed RTPDA detector finds all true corners without introducing any false corner. CPDA and fast-CPDA miss some true corners while GCM, SODC, Eigenvector, MSCP and RJ73 introduce some false corners.

5.2 Performance evaluation based on accuracy criterion

In this section, we present the evaluation performances based on accuracy criterion under Dataset 1. It should be pointed out that the thresholds of Canny edge detector are chosen as $low = 0$ and $high = 0.35$ following the setting in [33] and the "ground truth" corners are also from [33]. For a fair comparison, all compared detectors share the same Canny edge extraction and contour-tracking methods. Here we just select four typical contour-based detectors as reference ones: [4, 16, 29, 33]. The optimal parameters are summarized in Table 5 and the performances of the five compared detectors are shown in Table 6 and Fig. 10.

5.3 Some applications of the approach

Corner detection has many important applications on computer vision. Specially, since information about a shape is concentrated at the corners, they prove to be practical descriptive primitives in shape representation, objection recognition and motion analysis [30]. Figure 11 shows a practical application of our approach on the construction of shape descriptor. We first detect the corners of a shape and then extract all of the possible fragments defined by two corners with that the distance between the two points is more than 10 points. After that, each contour fragment is described (here we can choose an effective method, e.g. shape context [7]). Finally, we use K-means clustering algorithm to acquire the codebook of the contour fragments (all the shapes) and then derive the shape representation with a multi-dimensional vector, which can be conveniently applied to shape classification and shape recognition etc. In addition, we notice that Liu et al. [18–20] proposes to recognize activities from sensor data

where discriminant features are utilized. The attempt to replace the discriminant features with the features constructed with corners would be a very interesting work for us.

6 Conclusion and future work

In this paper, we presented a novel discrete curvature estimator based on *Relative Tangent-to-Point Distance Accumulation* (RTPDA) technique to provide a robust corner detection scheme. In RTPDA, we first fit the digital curve segments with quadratic polynomials by employing least square technique to derive the tangent of the target point and then compute the distance accumulation of its neighbors to the tangent. Based on the "discrete curvature", we developed a novel corner detection algorithm. Higher average repeatability and accuracy with relative low localization error compared with the-state-of-art contour-based corner detection algorithms demonstrate that it is a robust contour-based corner detector.

However, as a typical contour-based detector, RTPDA highly relies on the performances of edge-detection technique, which is a common problem suffered by boundary-based corner detection algorithms; besides, the discrete curvature of RTPDA detector is calculated under single-scale, while fusing multi-scale information may help RTPDA more robust. In the future, we would try to improve the performance of RTPDA algorithm based on the above two considerations and propose a more robust corner detection scheme.

Acknowledgments The work in this paper was partially supported by the National Natural Science Foundation of China (Grant no. 61602068), the Natural Science Foundation of Chongqing (Grant no. cstc2016jcyjA0458), the National Natural Science Foundation of China(Project No.81501548), the National Natural Science Foundation of China(Project No.61802352), the Fundamental Research Funds for the Central Universities (No.106112015CDJRC091101), the Henan Provincial Department of Science and Technology Research Project (172102210307) and Key Science Research Program of Henan Province (17A480004). The authors would like to thank the reviewers for their helpful suggestions and Dr. M. Awrangjeb for sharing his source code and Dataset 2.

References

1. Al Arif SMMR, Asad M, Gundry M (2017) Patch-based corner detection for cervical vertebrae in X-ray images. Signal Process Image Commun 59:27–36
2. Alzugaray I, Chli M (2018) Asynchronous corner detection and tracking for event cameras in real time. IEEE Robotics and Automation Letters 3(4):3177–3184
3. Awrangjeb M (2015). *Data set* [Online]. Available: http://users.monash.edu.au/~mawrangj/corner.html. Accessed 25 May 2015
4. Awrangjeb M, Lu G (2008) Robust image corner detection based on the chord-to-point distance accumulation technique. IEEE Transactions on Multimedia 10(6):1059–1072
5. Awrangjeb M, Lu G, Fraser CS, and Ravanbakhsh M (2009) A fast corner detector based on the chord-to point distance accumulation technique. Digital Image Computing: Techniques and Applications: 519–525
6. Awrangjeb M, Lu G, Fraser CS (2012) Performance comparisons of contour-based detectors. Transactions on Image Processing 21(9):4167–4179
7. Belongie S, Malik J, Puzicha J (2002) Shape matching and object recognition using shape contexts. IEEE Transactions on Pattern Analysis & Machine Intelligence 24:509–522
8. Canny J (1986) A computational approach to edge detection. IEEE Transactions on Pattern Analysis & Machine Intelligence 8(6):679–698
9. Chen S, Meng H, Zhang C (2016) A KD curvature based corner detector. Neurocomputing 173:434–441
10. Chen X, Liu L, Song J (2018) Corner detection and matching for infrared image based on double ring mask and adaptive SUSAN algorithm. Opt Quant Electron 50(4):194
11. Dellinger F, Delon J, Gousseau Y (2015) SAR-SIFT: a SIFT-like algorithm for SAR images. IEEE Trans Geosci Remote Sens 53(1):453–466

12. Ebrahimi S (2018) Vertebral corners detection on sagittal X-rays based on shape modelling, random forest classifiers and dedicated visual features. Computer Methods in Biomechanics and Biomedical Engineering: Imaging & Visualization:1–13
13. Harris C (1988) A Combined Corner and Edge Detector. Alvey Vision Conference: 147–151
14. He XC, Yung NHC (2008) Corner detector based on global and local curvature properties. Opt Eng 47: 057008
15. Lam SK, Lim TC, Wu M (2018) Area-time efficient FAST corner detector using data-path transposition. IEEE Transactions on Circuits and Systems II: Express Briefs 65(9):1224–1228
16. Lin X, Zhu C, Zhang Q (2017) Efficient and robust corner detectors based on second-order difference of contour. IEEE Signal Processing Letters 24(9):1393–1397
17. Lin X, Zhu C, Liu Y (2018) Robust corner detection using altitude to chord ratio accumulation. Multimedia Tools and Applications :1–19
18. Liu Y, Nie L, Han L (2015) Action2Activity: Recognizing Complex Activities from Sensor Data. In Twenty-fourth international joint conference on artificial intelligence: 1617–1623
19. Liu Y, Zhang L, Nie L (2016) Fortune Teller: Predicting Your Career Path. Thirtieth AAAI conference on artificial intelligence: 201–207
20. Liu Y, Nie L, Liu L (2016) From action to activity: sensor-based activity recognition. Neurocomputing 181: 108–115
21. Martínez-Sandoval E, Martínez-Rosas ME, de Ávila HC (2018) Method to extract an enhanced cervical vertebrae area from a digital X-ray image. Methodsx 5:752–760
22. Mohanna F, Mokhtarian F (2001) Performance evaluation of corner detection algorithms under similarity and affine transforms. In: Proceedings of the British Machine Vision Conference: 1–10
23. Mokhtarian F, Bober M (1998) Robust image corner detection through curvature scale space. IEEE Transactions on Pattern Analysis & Machine Intelligence 20(12):1376–1381
24. Mokhtarian F, Mohanna F (2006) Performance evaluation of corner detectors using consistency and accuracy measures. Comput Vis Image Underst 102(1):81–94
25. Moravec H P (1977) Toward automatic visual obstacle avoidance. International Joint Conference on Artificial Intelligence:584
26. Rosenfeld A, Johnston E (1973) Angle detection on digital curves. IEEE Trans Comput 22(9):875–878
27. Rosten E, Porter R, Drummond T (2010) Faster and better: a machine learning approach to corner detection. IEEE Trans Pattern Anal Mach Intell 32(1):105–119
28. Slabaugh GG, Knapp K, and Al-Arif SM (2017) Probabilistic Spatial Regression using a Deep Fully Convolutional Neural Network. British Machine Vision Conference: 4–7
29. Teng SW, Sadat RMN, Lu G (2015) Effective and efficient contour-based corner detectors. Pattern Recogn 48(7):2185–2197
30. Tsai DM, Hou HT, Su HJ (1999) Boundary-based corner detection using eigenvalues of covariance matrices. Pattern Recogn Lett 20:31–40
31. Yeh C-H (2003) Wavelet-based corner detection using eigenvectors of covariance matrices. Pattern Recogn Lett 24:2797–2806
32. Zhang X, Lei M, Yang D, Wang Y, Ma L (2007) Multi-scale curvature product for robust image corner detection in curvature scale space. Pattern Recogn Lett 28(5):545–554
33. Zhang X, Wang H, Smith AWB, Ling X, Lovell BC, Yang D (2010) Corner detection based on gradient correlation matrices of planar curves. Pattern Recogn 43(4):1207–1223
34. Zhang S, Yang D, Huang S (2015) Corner detection using arc length-based angle estimator[J]. Journal of Electronic Imaging 24(6):063010
35. Zhang S, Yang D, Huang S (2015) Corner detection using Chebyshev fitting-based continuous curvature estimation. Electron Lett 51(24):1988–1990
36. Zhang X, Qu Y, Yang D (2015) Laplacian scale-space behavior of planar curve corners. IEEE Transactions on Pattern Analysis & Machine Intelligence 37(11):2207–2217
37. Zhang S, Yang D, Huang S (2017) Robust corner detection using the eigenvector-based angle estimator. J Vis Commun Image Represent 45:181–193
38. Zhong B, Liao W (2007) Direct curvature scale space: theory and corner detection. IEEE Transactions on Pattern Analysis & Machine Intelligence 29(3):508–512

Shizheng Zhang received the B.S. degree from Zhengzhou University, Zhengzhou, China, in 2008 and the Ph.D. degree from Chongqing University, Chongqing, China, in 2016 respectively. His research interests include computer vision, pattern recognition and deep learning.

Sheng Huang received the B.Eng. degree in software engineering and the Ph.D. degree in computer science from Chongqing university, Chongqing, China, in 2010 and 2015, respectively. He was a visiting student in department of computer science at Rutgers university, Piscataway, NJ, USA, from 2012 to 2014. Currently, he is an associated professor in school of bigdata and software engineering at Chongqing university. He has authored around 30 scientific papers in venues, such as TIP, TIFS, CVPR, TCSVT, BMVC, ICIP. His research interests include pattern recognition, computer vision, machine learning, and biometrics.

Zhifeng Zhang received the B.S. degree from Xi'an Electronic and Science University, Xi'an, China, in 2001 and the M.S. degree from Xi'an University of Technology, Xi'an, China, in 2006 respectively. He was an associated professor of Zhengzhou University of Light Industry. His research interests include big data, cloud computing and machine learning.

Heng Wang received the B.S. degree from Henan Agricultural University in 2008, and received his M.S. and Ph.D. degrees in communication and information system from Chongqing University in 2012 and 2015, respectively. Now, he is an assistant professor with college of Mechanical and Electrical Engineering of Henan Agricultural University. His research interests cover advanced mobile communication systems and the key technologies, including heterogeneous network, green communications.

Junxia Ma received the B.S. degree from Henan Normal University, Xinxiang, China, in 1996 and the M.S. degree from Zhengzhou University, Zhengzhou, China, in 2007 respectively. She was an associated professor of Zhengzhou University of Light Industry. Her research interests include computer software theory, system safety and machine learning.

Pu Li received the B.S. degree from Tianjin Normal University, Tianjin, China, in 2006 and the Ph.D. degree from South China Normal University, Guangzhou, China, in 2017 respectively. His research interests include pattern recognition, machine learning and big data.